Eur. Phys. J. D **39**, 391–398 (2006)
DOI: 10.1140/epjd/e2006-00119-x

THE EUROPEAN PHYSICAL JOURNAL D

Relativistic R-matrix close-coupling calculations for photoionization of Ne-like Al IV

A.K.S. Jha[a], P. Jha[b], S. Tyagi, and M. Mohan[c]

Department of Physics and Astrophysics, University of Delhi, Delhi–110007, India

Received 9 January 2006 / Received in final form 3rd April 2006
Published online 7 June 2006 –

Abstract. We present relativistic close-coupling photoionization calculations of Al IV using the Breit-Pauli R-matrix method to obtain photoionization cross-section of Al IV from the ground state and the lowest two $J = 0$ (even) excited states. A multi-configuration eigenfunctions expansion of the core Al V is employed with spectroscopic configurations $2s^2 2p^5$, $2s2p^6$, $2s^2 2p^4 3s$, $2s^2 2p^4 3p$, $2s^2 2p^4 3d$ and $2s^2 2p^4 4s$. We have included, for the first time, the lowest 68 level target states of Al V in the photoionization calculations of Al IV. Extensive configuration interaction wavefunctions are used to describe both the initial Al IV states and the final Al V states. Cross-sections are compared from three level calculations including only $2s^2\ 2p^5\ {}^2\mathrm{P}^{\mathrm{o}}_{3/2,\ 1/2}$ and $2s\ 2p^6\ {}^2\mathrm{S}_{1/2}$ levels of Al V. The present calculation using the lowest 68 target levels of Al V are presented for the first time and should provide reasonably complete database for practical application for photoionization cross-section for Al IV, where high-energy cross-sections along with near-threshold photoionization cross-section is required.

PACS. 32.80.Fb Photoionization of atoms and ions

1 Introduction

In recent years there has been a considerable increase in the theoretical and experimental interest in the calculations of photoionization cross-section for positive ions, as these are needed for the interpretation of observational data for a wide variety of astronomical objects and laboratory plasmas [1]. With the ever increasing development of computational methods, on the theoretical side, close-coupling R-matrix method [2–5] has become the most accurate tool for ab-initio calculations of low energy electron collision processes involving atoms and ions, as it takes important physical effects like exchange, channel coupling and short range correlations into account. On the experimental side, this has been stimulated by the ready availability of synchrotron radiations sources enabling accurate measurements to be carried out over the whole spectral range from the visible to the X-ray region. Two decade ago Lyon et al. [6,7] made the first absolute measurements of photoionization cross-section of atomic ions using merged beam technique. Experimental facilities aimed at measuring absolute photoionization cross-section for singly and multiply ionized ions have been developed around the world e.g. at Paris (LURE), Tsukuba (Photon Factory), Aarhus (ASTRID) and Berkeley (ALS). Thus, the availability of accurate experimental data from various sources around the world is now stimulating urgent need of accurate theoretical calculations for comparison.

The photoionization of aluminum has been previously considered by several theoretical and experimental groups [8]. West et al. [9] have discussed in detail the partial Al^+ photoionization cross-section for the production of Al^{2+} and Al^{3+} and the total photoionization cross-section in the photon energy region 80–160 eV. High-resolution photoionization cross-section measurement has been made at the ALS, corresponding to the $2p$ excitation of the Al II ground state, in photon energy >80 eV [10]. Chakraborty et al. [11] have calculated near-threshold photoionization cross-section for Al IV and found the Al IV cross-section almost flat at threshold but gradually dominated by inner-shell $2s \rightarrow 3p$ resonance which moved down in energy to within ∼13 eV of the threshold. Recently, Kochur et al. have produced Al II, Al III and Al IV lines using soft X-ray irradiation on atomic aluminium and presented photoionization of $2s$-, $2p$-, and $3s$-subshells in the photon energy range from 80 eV to 1 keV [12].

Neon-like Al IV ion has attracted much attention during the last quarter of century. Kaufman et al. [13] and Artru and Kaufman [14] predicted wavelengths for almost 300 Al IV lines from 476 to 4626 Å. Resonance transitions of the type $2p^6\ {}^1\mathrm{S}_0 \rightarrow 2p^5 nd$ ($J = 1$) were observed to $6d$ by Soderqvist [15] and to $7d$ by Jamelot et al. [16]. Further, absorption features in the range 75–100 Å have been

[a] e-mail: aloksinghjha@yahoo.co.in
[b] e-mail: pkjha@physics.du.ac.in
[c] e-mail: sneh@del2.vsnl.net.in

observed in the spectra of laser-produced Al plasmas [17] and high-voltage sparks by Kastner et al. [18]. They have reported the autoionizing transitions of $2s^22p^6 \rightarrow 2s2p^6np$ in neon like Al IV and predicted the wavelengths of the first member of the series to be near 95.1 Å in Al IV. The detailed analysis of spectrograms of Ne isoelectronic sequence including Al IV [19] has provided a detailed knowledge of the energy levels of principle quantum number $n = 3$ for Ne isoelectronic sequence including Al IV and the precise position of these levels has allowed Fawcett [20] to calculate weighted oscillator strengths for the ions in the isoelectronic sequence between Al IV and Ar IX. Soderqvist and Ferner [21] classified most of the Al V lines in the region 85–282 Å where as, 140 new lines were remeasured in the region below 300 Å by Artru and Brillet [22]. Further, Brillet and Artru [23] added 96 lines of Al V in the range 456–1621 Å.

Neon-like aluminum ions are of crucial importance in many astrophysical applications e.g. in the calculation of opacity of steller envelops. Neon-like aluminum ions produced by z-pinch plasma were used in vacuum ultra-violet lasing by Rahmani et al. [24]. In the X-ray laser research, photoionization of neon-like ions has found applications in understanding the resonant photo-pumping scheme for driving lasing action [25]. Photoionization of the neon-like ions, aside from its importance as the response of the simplest noble gas structure with multiple shells to ionization radiation, is also of particular interest owing to the significant cosmic abundance [26]. Apart from practical needs, neon-like ions has also attracted theoretical interest because of both the simplicity and complexity of the particle-hole states of closed-shell ions.

We have applied relativistic close coupling R-matrix method for the photoionization cross-section from the ground state $1s^22s^22p^6\ ^1\mathrm{S}_0$ and the lowest two $J = 0$ (even) excited states of Al IV by including, for the first time, the lowest 68 fine-structure levels of Al V as target states. The primary driving force behind our extensive 68 state calculation comes from the fact that the near threshold photoionization cross-section is inadequate for practical applications, which also require the higher-energy cross-sections for modeling ionization balance in laboratory and astrophysical plasmas. Further, a three-level calculation gives little indication of the complexity of the cross-section. In our present calculation we have performed two sets of calculations, one involving only the lowest three target states while the other one has been done by taking the lowest 68 fine structure levels of Al V as target states. Comparison between two indicates that below the $n = 2$ thresholds there is little a difference between the two sets of calculations.

2 Calculations

The relativistic R-matrix method is used to obtain photoionization cross-section of Al IV from its ground state $1s^22s^22p^6\ ^1\mathrm{S}^\mathrm{e}$, $J = 0$ and lowest two $J = 0$ (even) excited states. Relativistic effects have been taken by including Breit-Pauli interactions in the Hamiltonian i.e. mass-correction term, one-electron Darwin term and spin-orbit term [4]. In the R-matrix formulation of photoionization the initial bound state of Al IV and the final continuum states of the residual consistently is collisional type R-matrix basis sets, are expressed in terms of the states of N-electron residual ion Al V. The wave functions used for the Al V target states are represented by intermediate coupling LSJ configuration expansion [27] as:

$$\Phi\left(J\right) = \sum_{i=1}^{M} a_i \varphi_i\left(\alpha_i, LSJ\right) \tag{1}$$

where the single configuration function φ_i are constructed from one electron orbitals, whose angular momenta are coupled as specified by α_i to form states of given total L, S and J. These target states are represented by configuration interaction (CI) wave function described in detail by Mohan and Hibbert [28]. The radial part of each orbital is written as a linear combination of normalized slater-type orbitals (STOS)

$$P_{n\ell}(r) = \sum_{i=1}^{k} C_i\, r^{p_i} \exp(-\zeta_i r). \tag{2}$$

The parameters $\{C_i\}$, $\{p_i\}$ and $\{\zeta_i\}$ in equation (2) are determined variationally as described by Hibbert, Mohan and Le Dourneuf [29]. We have used eight orthogonal orbitals ($1s$, $2s$, $2p$, $3s$, $3p$, $3d$, $4s$, $4p$). The radial functions for $1s$ and $2s$ were taken to be the Hartree-Fock orbitals of Clementi and Roetti [30] while, the radial functions for $2p$, $3s$, $3p$, $3d$ and $4p$ have been taken from Blackford et al. [31]. Finally, $4s$ orbital is optimized on excited state $2p^4\ 4s\ ^2\mathrm{S}^\mathrm{e}$. In Table 1, we have listed the configurations used in the CI expansion of the Al V target states, where as in Table 2 we have compared our excitation energies (relative to the ground state) of fine-structure levels of Al V, with the latest available NIST [32] energy table. Energy difference between our results and NIST is due to lesser number of configurations included in the present calculation for doing manageable scattering calculations. The level of configuration interaction [33] is less than we would like but further inclusion of this future would require substantially increased computer resources.

We have represented the lowest 68 LSJ states of Al V included in the calculation as described by equation (1). The energies of the corresponding states in the Breit-Pauli approximation are defined by

$$\left\langle \Phi_i\left(J\right) \left| H_{BP}^{N} \right| \Phi_{i'}\left(J'\right) \right\rangle = E_i^N \delta_{ii'} \delta_{JJ'} \tag{3}$$

where we have included the mass-correction, one body Darwin and spin-orbit terms in the Breit-Pauli Hamiltonian H_{BP}^N

$$H_{BP}^N = H_{NR}^N + H_{mass}^N + H_{DI}^N + H_{SO}^N$$

Table 1. Configurations use in CI expansion of Al V target state.

Key No.	State		Configuration used
1	$2s^2\ 2p^5$	^{2}P$^\circ$	$2s^22p^5$, $2s^22p^4(^3\mathrm{P})3p$, $2s^22p^4(^1\mathrm{D})3p$, $2p^4(^1\mathrm{S})3p$
2	$2s\ 2p^6$	^{2}S$^\mathrm{e}$	$2s2p^6$, $2s^22p^4(^1\mathrm{S})3s$, $2s^2\ 2p^4(^1\mathrm{D})3d$, $2s^22p^4(^1\mathrm{S})4s$
3	$2s^2\ 2p^4(3p)3s$	^{4}P$^\mathrm{e}$	$2s^22p^4(3p)3s$, $2s^22p^4(3p)3d$, $2s^2\ 2p^4(3p)4s$
4	$2s^2\ 2p^4(3p)3s$	^{2}P$^\mathrm{e}$	$2s^22p^4(3p)3s$, $2s^22p^4(3p)3d$, $2s^22p^4(^1\mathrm{D})3d$, $2s^22p^4(3p)4s$
5	$2s^2\ 2p^4(^1\mathrm{D})3s$	^{2}D$^\mathrm{e}$	$2s^22p^4(^1\mathrm{D})3s$, $2s^22p^4(3p)3d$, $2s^22p^4(^1\mathrm{D})3d$, $2s^22p^4(^1\mathrm{D})4s$
6	$2s^2\ 2p^4(3p)3p$	^{4}P$^\circ$	$2s^2\ 2p^4(3p)3p$
7	$2s^2\ 2p^4(3p)3p$	^{4}D$^\circ$	$2s^2\ 2p^4(3p)3p$
8	$2s^2\ 2p^4(3p)3p$	^{2}D$^\circ$	$2s^22p^4(3p)3p$, $2s^2\ 2p^4(^1\mathrm{D})3p$
9	$2s^2\ 2p^4(3p)3p$	^{2}S$^\circ$	$2s^2\ 2p^4(3p)3p$
10	$2s^2\ 2p^4(3p)3p$	^{4}S$^\circ$	$2s^2\ 2p^4(3p)3p$
11	$2s^2\ 2p^4(3p)3p$	^{2}F$^\circ$	$2s^2\ 2p^4(^1\mathrm{D})3p$
12	$2s^2\ 2p^4(3p)3d$	^{4}D$^\mathrm{e}$	$2s^2\ 2p^4(3p)3d$
13	$2s^2\ 2p^4(3p)3d$	^{4}F$^\mathrm{e}$	$2s^2\ 2p^4(3p)3d$
14	$2s^2\ 2p^4(3p)3d$	^{2}F$^\mathrm{e}$	$2s^2\ 2p^4(3p)3d$, $2s^2\ 2p^4(^1\mathrm{D})3d$
15	$2s^2\ 2p^4(^1\mathrm{D})3d$	^{2}G$^\mathrm{e}$	$2s^22p^4(^1\mathrm{D})3d$

with

$$H^N_{mass} = -\frac{1}{8}\alpha^2 \sum_{i=1}^{N} \nabla_i^4,$$

$$H^N_{DI} = -\frac{1}{8}\alpha^2 Z \sum_{i=1}^{N} \nabla_i^2 \left(\frac{1}{r_i}\right),$$

$$H^N_{SO} = \frac{1}{2}\alpha^2 Z \sum_{i=1}^{N} \frac{\overrightarrow{l_i}.\overrightarrow{s_i}}{r_i^3}.$$

As described by Burke and Taylor [34], in the R-matrix theory of photoionization, both the initial bound state and the final continuum state $\psi_f(\vec{k})$ are expanded in terms of discrete R-matrix basis sets

$$\psi_k = \mathrm{A} \sum_{ij} C_{ijk} \Phi_i \left(X_1 X_2 \ldots X_N; \hat{r}_{N+1}, \sigma_{N+1}\right) u_{ij}\left(r_{N+1}\right) + \sum_j d_{jk} \varphi_j (X_1 \ldots X_{N+1}) \quad (4)$$

inside a sphere of radius 'a' containing the charge distribution of the residual ion. In (4), A is the antisymmetrisation operator which accounts for electron exchange, Φ_i are channel functions formed by coupling the target states of coordinates $\mathrm{X}_i = \{r_i, \hat{r}_i, \sigma_i\}$ with the spin angle function of the scattered electron in order to form eigenstate of the total angular momentum J_t and parity Π_t.

More precisely, following Scott and Burke [34], the pair-coupling scheme is used,

$$\vec{J} + \vec{l} = \vec{K}, \qquad \vec{K} + 1/2 = \vec{J} \quad (5)$$

since this coupling scheme is expected to be approximately realized in medium size atomic systems. The (u_{ij}) form a discrete R-matrix basis of continuum orbitals for the scattered electron and the $\{\Phi_j\}$ are $\{N+1\}$-electron bound configuration, which account for the orthogonality of the continuum orbitals u_{ij} to the bound orbitals.

The continuum orbitals u_{ij} in (4) are eigenfunctions of a zero-order non-relativistic model Hamiltonian, which satisfy the boundary conditions:

$$u_{ij}(0) = 0, \quad (6)$$

$$\frac{a}{u_{ij}} \frac{\mathrm{d}u_{ij}}{\mathrm{d}r}\bigg|_{r=a} = b. \quad (7)$$

We imposed a zero logarithmic derivative $b = 0$ at the R-matrix boundary radius 'a' and we retained 15 continuum orbitals for each angular symmetry to ensure convergence in the energy range considered here. The coefficients C_{ijk} and d_{jk} in (4) were determined by diagonalising the $(N+1)$-electron Breit-Pauli Hamiltonian matrix (Eq. (3) for $N+1$ electrons) in the inner region. In the outer region ($r > a$) the radial equations were solved, assuming a purely Coulombic asymptotic interaction.

In R-matrix theory, we partition configuration space into two regions by a sphere of radius 'a' centered on the center of mass and chosen in such a way as to effectively enclose the target electrons [35]. In the external region $r > a$, electron exchange between the scattered electron and target can be neglected if the radius a is chosen large enough so that the charge distribution of the target is contained within the sphere. We have chosen the radius of sphere 'a' defining the internal region so that the functions Φ_i and φ_j (in Eq. (4)) are effectively zero when $r > a$ and thus channel coupling can be ignored in this region [5]. Therefore, the N electron target orbitals must become vanishingly small in the external region. The boundary radius 'a' is chosen in the external region such that $|P_{nl}(r = a)| < \delta$ for all bound orbitals included in the calculations, where δ is a small number e.g. of the order of 10^{-4} a.u.

Finally, the differential cross-section for photoionization of an $(N+1)$-electron atom with the electron ejected

Table 2. Fine-structure energy levels (in Rydbergs) for the 68CC eigenfunction expansion of the target ion Al V compared to the NIST.

I	Configuration	Term	$2J$	E (Present)	E (NIST)
1	$2s2p^5$	^{2}P°	3	0.00000	0.00000
2			1	0.03914	0.03137
3	$2s2p^6$	^{2}S	1	3.45845	3.26977
4	$2s\ ^2 2p^4(^3\mathrm{P})3s$	^{4}P	5	6.77759	6.85127
5			3	6.80059	6.87086
6			1	6.81484	6.88223
7	$2s\ ^2 2p^4(^3\mathrm{P})3s$	^{2}P	3	6.88811	6.96436
8			1	6.91579	6.98753
9	$2s\ ^2 2p^4(^1\mathrm{D})3s$	^{2}D	5	7.20366	7.25936
10			3	7.20393	7.25964
11	$2s\ ^2 2p^4(^3\mathrm{P})3p$	^{4}P°	5	7.35830	7.44838
12			3	7.36861	7.45541
13			1	7.37478	7.46293
14	$2s^2 2p^4(^3\mathrm{P})3p$	^{4}D°	7	7.41488	7.52485
15			5	7.42945	7.53641
16			3	7.43985	7.54561
17			1	7.44609	7.55063
18	$2s\ ^2 2p^4(^3\mathrm{P})3p$	^{2}D°	5	7.51080	7.58190
19			3	7.53608	7.60074
20	$2s\ ^2 2p^4(^3\mathrm{P})3p$	^{2}P°	1	7.53655	7.60938
21			3	7.58216	7.62674
22	$2s\ ^2 2p^4(^3\mathrm{P})3p$	^{4}S°	3	7.55690	7.63319
23	$2s\ ^2 2p^4(^3\mathrm{P})3s$	^{2}S°	1	7.55692	7.63749
24	$2s\ ^2 2p^4(^1\mathrm{S})3s$	^{2}S	1	7.76830	7.69031
25	$2s\ ^2 2p^4(^1\mathrm{D})3p$	^{2}F°	5	7.83532	7.88582
26			7	7.83924	7.88961
27	$2s\ ^2 2p^4(^1\mathrm{D})3p$	^{2}D°	3	7.90901	7.96471
28			5	7.91129	7.96703
29	$2s\ ^2 2p^4(^1\mathrm{D})3p$	^{2}P°	1	7.99737	8.06648
30			3	8.01798	8.05158
31	$2s\ ^2 2p^4(^3\mathrm{P})3d$	^{4}D	7	8.22659	8.30141
32			5	8.22992	8.30464
33			3	8.23453	8.30875
34			1	8.23867	8.31224
35	$2s\ ^2 2p^4(^3\mathrm{P})3\mathrm{d}$	^{4}F	9	8.28417	8.36190
36			7	8.29699	8.37233
37			5	8.30872	8.38275
38			3	8.31662	8.38981
39	$2s\ ^2 2p^4(^3\mathrm{P})3d$	^{2}F	7	8.32634	8.39345
40			5	8.34526	8.40740
41	$2s\ ^2 2p^4(^3\mathrm{P})3d$	^{4}P	1	8.32184	8.39656
42			3	8.33019	8.40309
43			5	8.34082	8.41307
44	$2s\ ^2 2p^4(^3\mathrm{P})3d$	^{2}D	3	8.36987	8.43316
45			5	8.38193	8.44187
46	$2s\ ^2 2p^4(^3\mathrm{P})3d$	^{2}P	1	8.37083	8.43737
47			3	8.39976	8.46028
48	$2s\ ^2 2p^4(^1\mathrm{S})3p$	^{2}P°	1	8.40941	8.35999
49			3	8.44784	8.36054
50	$2s\ ^2 2p^4(^1\mathrm{D})3d$	^{2}G	7	8.65209	8.70944
51			9	8.65281	8.70948
52	$2s\ ^2 2p^4(^1\mathrm{D})3d$	^{2}P	3	8.70393	8.75607
53			1	8.70970	8.76309
54	$2s\ ^2 2p^4(^1\mathrm{D})3d$	^{2}S	1	8.71575	8.75195
55	$2s\ ^2 2p^4(^1\mathrm{D})3d$	^{2}F	7	8.72427	8.77873
56			5	8.72437	8.77877
57	$2s\ ^2 2p^4(^1\mathrm{D})3d$	^{2}D	5	8.72554	8.77214
58			3	8.73032	8.77841
59	$2s\ ^2 2p^4(^3\mathrm{P})4s$	^{4}P	5	9.02953	9.12258
60			3	9.04779	9.13934
61			1	9.06602	9.15321
62	$2s\ ^2 2p^4(^3\mathrm{P})4s$	^{2}P	3	9.07330	9.16543
63			1	9.09690	9.18624
64	$2s\ ^2 2p^4(^1\mathrm{S})3d$	^{2}D	5	9.25978	9.17779
65			3	9.26100	9.17910
66	$2s\ ^2 2p^4(^1\mathrm{D})4s$	^{2}D	5	9.43316	9.50898
67			3	9.43326	9.50903
68	$2s\ ^2 2p^4(^1\mathrm{S})4s$	^{2}S	1	9.99887	9.93242

in direction $\vec{k}$ and the ion left in state f is given by [34]

$$\frac{d\sigma_f}{d\vec{k}} = 8\Pi^2 \alpha a_0^2 \omega \left| \left\langle \psi_{\vec{f}}\left(\vec{k}\right) \left| \sum_{i=1}^{N+1} \vec{r}_i \right| \psi_i \right\rangle \right|^2 \qquad (8)$$

where ω is the photon energy in a.u., α is the fine structure constant, a_0 is the Bohr radius, ψ_i is the wavefunction of the initial bound state and $\psi_{\vec{f}}(\vec{k})$ is the wavefunction of the final state with a single outgoing wave corresponding to the ejected electron in direction $\vec{k}$ and the residual ion in state f.

3 Result and discussion

The following section present extensive results for photoionization cross-section of Al IV from its ground state and lowest two $J = 0$ (even) excited states. The three-level calculations are compared with the 68-level cases. Three-level calculations include only the $n = 2$ levels while the 68-level calculations include most of the $n = 3$ complex along with eight fine structure target levels of $n = 4$ complex. For the target state we have included 15 parities, namely, ^{2}S°, ^{2}P°, ^{2}D°, ^{2}F°, ^{4}S°, ^{4}P°, ^{4}D°, ^{2}S, ^{2}P, ^{2}D, ^{2}F, ^{2}G, ^{4}P, ^{4}D and ^{4}F, to obtain photoionization of Al IV from ground state $2s^2 2p^6\ ^1\mathrm{S}_0$. The target includes doublets and quartets, which allows the $(N + 1)$ configuration to be singlets, triplet or quintets. In case of photoionization of Al IV from ground state $2s^2 2p^6\ ^1\mathrm{S}_0$, Al V ion plus electron will combine to give symmetry of ^{1}P°. We are considering here only one transition i.e. $J = 0 \rightarrow 1°$. Applying the Illegal variable name. condition $|J - S| \leq L \leq |J + S|$ to the $(N + 1)$ values of $S = 0$, 1, 2 and taking care of dipole selection rule, we have included the following possible transitions; $^1\mathrm{S}_0 \rightarrow {}^1\mathrm{P}^\circ_1$, $^3\mathrm{P}_0 \rightarrow {}^3\mathrm{S}^\circ_1$, $^3\mathrm{P}^\circ_1$, $^3\mathrm{D}^\circ_1$ and $^5\mathrm{D}_0 \rightarrow {}^5\mathrm{P}^\circ_1, {}^5D^\circ_1, {}^5F^\circ_1$. The present calculation evaluate photoionization

cross-section for the following processes:

$$\mathrm{Al\,IV}\left(1s^2 2s^2 2p^6\ {}^1\mathrm{S}, J=0\right)+h\nu \rightarrow |\mathrm{Al\,V}\left(1s^2 2s^2 2p^5\ {}^2\mathrm{P}^\circ_{3/2,1/2}\right)+e^-(s,d)|, \quad J=1^\circ \tag{9a}$$

$$\mathrm{Al\,IV}\left(1s^2 2s^2 2p^6\ {}^1\mathrm{S}, J=0\right)+h\nu \rightarrow |\mathrm{Al\,V}\left(1s^2 2s^2 2p^6\ {}^2\mathrm{S}_{1/2}\right)+e^-(p)|, \quad J=1^\circ \tag{9b}$$

$$\mathrm{Al\,IV}\left(1s^2 2s^2 2p^6\ {}^1\mathrm{S}, J=0\right)+h\nu \rightarrow |\mathrm{Al\,V}\left(1s^2 2s^2 2p^4({}^3\mathrm{P})3s^4\mathrm{P}^2_{5/2,3/2,1/2,}\mathrm{P}^2_{3/2,1/2}\right)+e^-(p,f)|, \quad J=1^\circ \tag{9c}$$

$$\mathrm{Al\,IV}\left(1s^2 2s^2 2p^6\ {}^1\mathrm{S}, J=0\right)+h\nu \rightarrow |\mathrm{Al\,V}\left(1s^2 2s^2 2p^4({}^1\mathrm{D})3s^2\mathrm{D}_{5/2,3/2}\right)+e^-(p,f)|, \quad J=1^\circ \tag{9d}$$

$$\mathrm{Al\,IV}\left(1s^2 2s^2 2p^6\ {}^1\mathrm{S}, J=0\right)+h\nu \rightarrow |\mathrm{Al\,V}(1s^2 2s^2 2p^4({}^3\mathrm{P})3p^4\mathrm{P}^\circ_{5/2,3/2,1/2,}\ {}^4\mathrm{D}^\circ_{7/2,5/2,3/2,1/2,}\ {}^2\mathrm{D}^\circ_{5/23/2},\ {}^2\mathrm{P}^\circ_{1/2,3/2,}\ {}^4\mathrm{S}^\circ_{3/2,}\ {}^2\mathrm{S}^\circ_{1/2}+e^-(s,d,g)|, \quad J=1^\circ \tag{9e}$$

$$\mathrm{Al\,IV}\left(1s^2 2s^2 2p^6\ {}^1\mathrm{S}, J=0\right)+h\nu \rightarrow |\mathrm{Al\,V}\left(1s^2 2s^2 2p^4({}^1\mathrm{S})3s^2\mathrm{S}_{1/2}\right)+e^-(p)|, \quad J=1^\circ \tag{9f}$$

$$\mathrm{Al\,IV}\left(1s^2 2s^2 2p^6\ {}^1\mathrm{S}, J=0\right)+h\nu \rightarrow |\mathrm{Al\,V}\left(1s^2 2s^2 2p^4({}^1\mathrm{D})3p^2\mathrm{F}^\circ_{5/2,7/2}\ {}^2\mathrm{D}^\circ_{3/2,5/2,}\ {}^2\mathrm{P}^\circ_{1/2,3/2,}\right)+e^-(s,d,g)|, \quad J=1^\circ \tag{9g}$$

$$\mathrm{Al\,IV}\left(1s^2 2s^2 2p^6\ {}^1\mathrm{S}, J=0\right)+h\nu \rightarrow |\mathrm{Al\,V}\left(1s^2 2s^2 2p^4({}^3\mathrm{P})3d\ {}^4\mathrm{D}_{7/2,5/2,3/2,1/2}\ {}^4\mathrm{F}_{9/2,7/2,5/2,3/2,}\ {}^2\mathrm{F}_{7/2,5/2,}\ {}^4\mathrm{P}_{1/2,3/2,5/2,}\ {}^2\mathrm{D}_{3/2,5/2,}\ {}^2\mathrm{P}_{1/2,3/2}\right)+e^-(p,f,h)|, \quad J=1^\circ \tag{9h}$$

$$\mathrm{Al\,IV}\left(1s^2 2s^2 2p^6\ {}^1\mathrm{S}, J=0\right)+h\nu \rightarrow |\mathrm{Al\,V}\left(1s^2 2s^2 2p^4({}^1\mathrm{S})3p^2\mathrm{P}^\circ_{1/2,3/2,}\right)+e^-(s,d)|, \quad J=1^\circ \tag{9i}$$

$$\mathrm{Al\,IV}\left(1s^2 2s^2 2p^6\ {}^1\mathrm{S}, J=0\right)+h\nu \rightarrow |\mathrm{Al\,V}\left(1s^2 2s^2 2p^4({}^1\mathrm{D})3d\ {}^2\mathrm{G}_{7/2,9/2,}\ {}^2\mathrm{P}_{3/2,1/2,}\ {}^2\mathrm{S}_{1/2,}\ {}^2\mathrm{F}_{7/2,5/2,}\ {}^2\mathrm{D}_{5/2,3/2}\right)+e^-(p,f,h)|, \quad J=1^\circ \tag{9j}$$

$$\mathrm{Al\,IV}\left(1s^2 2s^2 2p^6\ {}^1\mathrm{S}, J=0\right)+h\nu \rightarrow |\mathrm{Al\,V}(1s^2 2s^2 2p^4({}^3\mathrm{P})4s^4\mathrm{P}_{5/2,3/2,1/2,}\ {}^2\mathrm{P}_{3/2,1/2}+e^-(p,f)|, \quad J=1^\circ \tag{9k}$$

$$\mathrm{Al\,IV}(1s^2 2s^2 2p^6\ {}^1\mathrm{S}, J=0)+h\nu \rightarrow |\mathrm{Al\,V}(1s^2 2s^2 2p^4({}^1\mathrm{S})3d^2\mathrm{D}_{5/2,3/2})+e^-(p,f)|, \quad J=1^\circ \tag{9l}$$

$$\mathrm{Al\,IV}\left(1s^2 2s^2 2p^6\ {}^1\mathrm{S}, J=0\right)+h\nu \rightarrow |\mathrm{Al\,V}(1s^2 2s^2 2p^4({}^1\mathrm{D})4s\ {}^2\mathrm{D}_{5/2,3/2}+e^-(p,f)|, \quad J=1^\circ \tag{9m}$$

$$\mathrm{Al\,IV}\left(1s^2 2s^2 2p^6\ {}^1\mathrm{S}, J=0\right)+h\nu \rightarrow |\mathrm{Al\,V}(1s^2 2s^2 2p^4({}^1\mathrm{S})4s^2\mathrm{S}_{1/2}+e^-(p)|, \quad J=1^\circ \tag{9n}$$

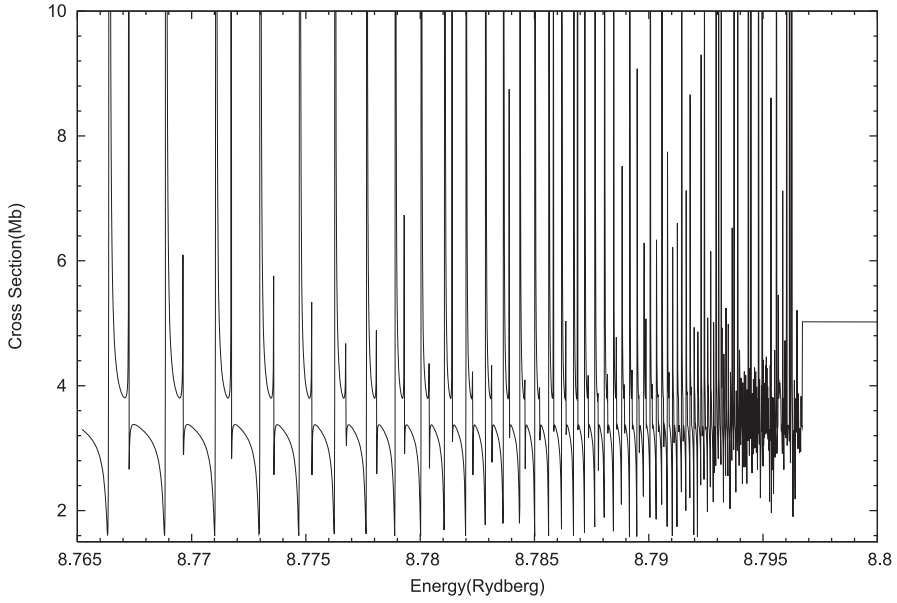

Fig. 1. Photoionization cross-section in Mb for the photoionization from the ground state of Al IV in relativistic *LSJ* coupling as a function of photon energy in the energy region from 8.765 Rydberg ($2s^2 2p^5\ {}^2\mathrm{P}^\circ_{3/2}$ threshold of Al V) to 8.8 Rydberg (just above $2s^2 2p^5\ {}^2\mathrm{P}^\circ_{1/2}$ threshold of Al V).

In Figure 1, we have shown the cross-section for the photoionization of ground state $2s^2 2p^6\ {}^1\mathrm{S}_0$ of Al IV in the photon energy range from ${}^2\mathrm{P}^\circ_{3/2}$ threshold to near the first excited threshold ${}^2\mathrm{P}^\circ_{1/2}$ of Al V, depicted by equation (9a). Here we find resonances due to two sets of Rydberg series $2s^2 2p^5\ {}^2\mathrm{P}^\circ_{1/2}\{ns[1/2]_1,\ nd[3/2]_1\}$, converging to the near ${}^2\mathrm{P}^\circ_{1/2}$ threshold of Al V. This is a pure relativistic effect and will not appear in the non-relativistic calculation as ${}^2\mathrm{P}^\circ$ represents only one state in *LS* coupling [36]. This region of cross-section is dominated by autoionizing resonances which corresponds to the transition $2s^2 2p^6\ {}^1\mathrm{S}_0 \rightarrow 2s^2 2p^5\ {}^2\mathrm{P}^\circ_{1/2}\ \{ns[1/2]_1,\ nd[3/2]_1\}$ which arises from ionization of the $2p$ electron into the continuum. Here, we have used the the *JLK* coupling scheme, which is programmed in the Breit-Pauli R-matrix codes.

In Figure 2, we have plotted photoionization cross-section for the ground state $2s^2 2p^6\ {}^1\mathrm{S}_0$ in the photon energy range 10.5 Rydberg to 12.5 Rydberg, near $2s2p^6\ {}^2\mathrm{S}_{1/2}$ threshold of Al V. This region is dominated

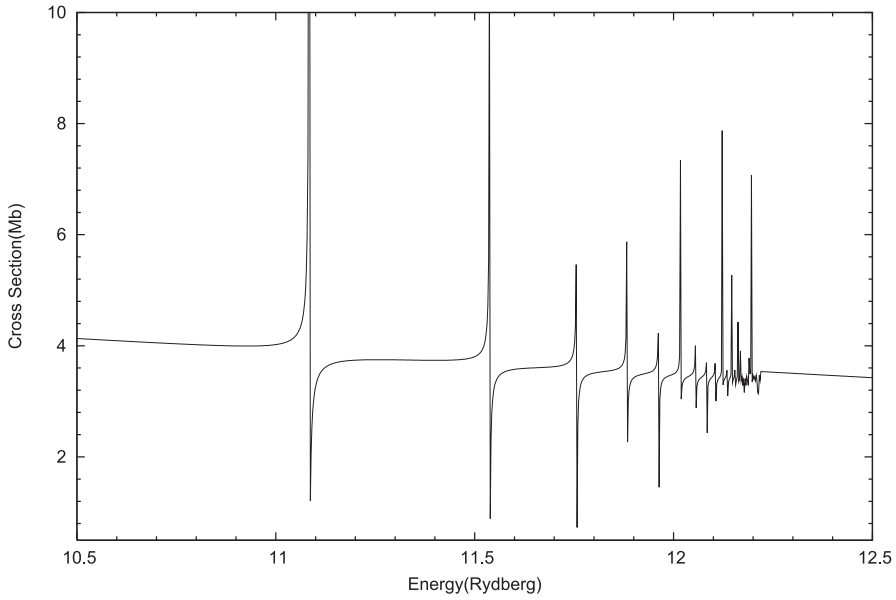

Fig. 2. Photoionization cross-section in Mb for the photoionization from the ground state of Al IV as a function of photon energy in the energy region from 10.5 Rydberg to 12.5 Rydberg (just above $2s2p^6\ ^2S_{1/2}$ threshold of Al V).

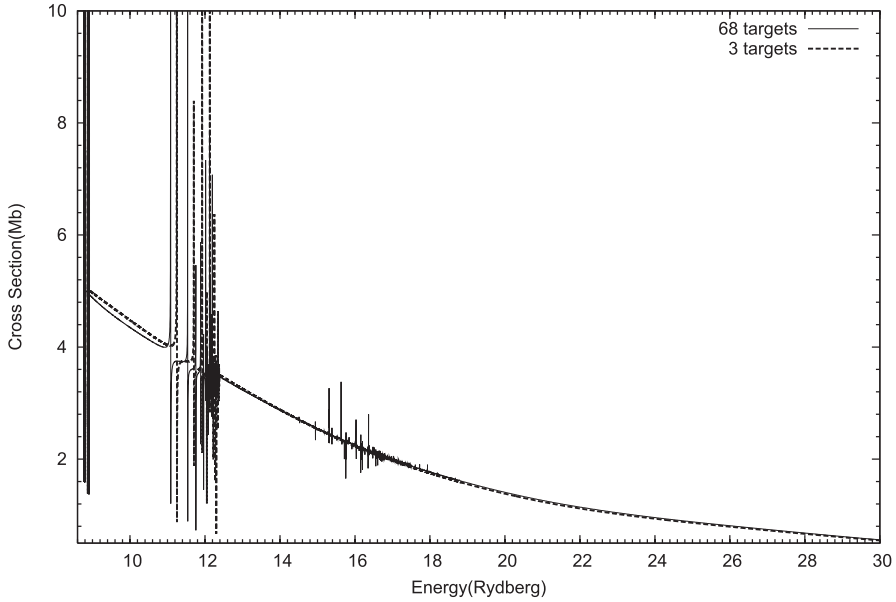

Fig. 3. Comparison of photoionization cross-section in Mb of Al IV from its ground state by taking the lowest 68 and 3 targets of Al V for full range upto 30 Rydberg. Dotted lines represents calculations taking the lowest 3 targets while solid line represents calculations by taking the lowest 68 targets of Al V.

by closed (or Fesbach) resonances which perturb the otherwise smoothly varying cross-section. The inner-shell resonances $2s \rightarrow \{np[1/2]_1,\ np[3/2]_1\}$ corresponding to equation (9b), gives rise to the Rydberg series $2s2p^6\ ^2S_{1/2}\{np[1/2]_1,\ np[3/2]_1\}$, which converge to near $^2S_{1/2}$ threshold of Al V.

Figure 3, shows comparison of photoionization cross-section for the ground state of Al IV between the three level calculation and 68 level calculations, with similar resolution. The dotted lines represent calculations taking the lowest 3 targets while the solid line represents calculations by taking the lowest 68 targets of Al V. The ionization potential for 68 level calculation is 8.7652 Rydberg, which is reasonably close to experimental ionization potential which is 8.8193 Rydberg. The ground-level photoionization cross-section of Al IV is not greatly affected by the $n = 3$ complexes of resonances. We can clearly see that below the $2s2p^6\ ^2S_{1/2}$ threshold of Al IV, there is little difference between the two. However, around 15 Rydberg we find lot of resonances appearing in 68 level calculations which arise due to the resonances converging to the thresholds from $2s^22p^4(^3P)3s\ ^4P_{5/2,3/2,1/2}$ to $2s^22p^4(^1S)4s\ ^2S_{1/2}$ of Al V.

In Figures 4 and 5, we have displayed the present result for the photoionization of Al IV from the $2s^22p^5(^2P^\circ)3p\ ^3P_0$ and $2s^22p^5(^2P^\circ)3p\ ^1S_0$ state respectively. For these state same Rydberg series are possible as those for the photoionization from $2s^22p^6\ ^1S_0$ state. Ionization potential for the $2s^22p^5(^3P^\circ)3p\ ^3P_0$ state is 2.411627 Rydberg while for the $2s^22p^5(^3P^\circ)3p\ ^1S_0$ state, the ionization potential is 2.140351 Rydberg. In the case of excited levels the $n = 3$ complexes of resonances

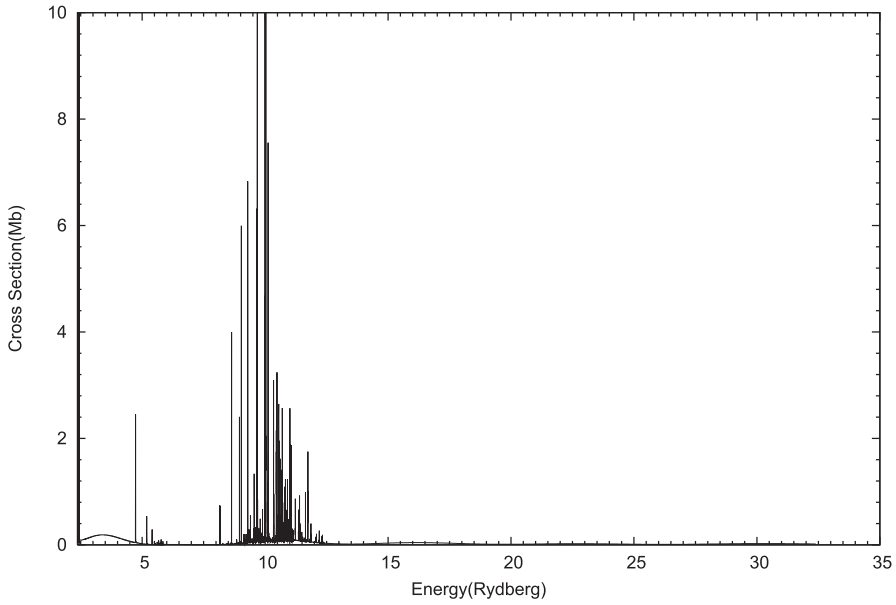

Fig. 4. Photoionization cross-section in Mb for the photoionization from $2s^2 2p^5(^2\mathrm{P}^\circ)3p\ ^3\mathrm{P}_0$ state of Al IV in Relativistic LSJ coupling as a function of photon energy in the full range upto 35 Rydberg.

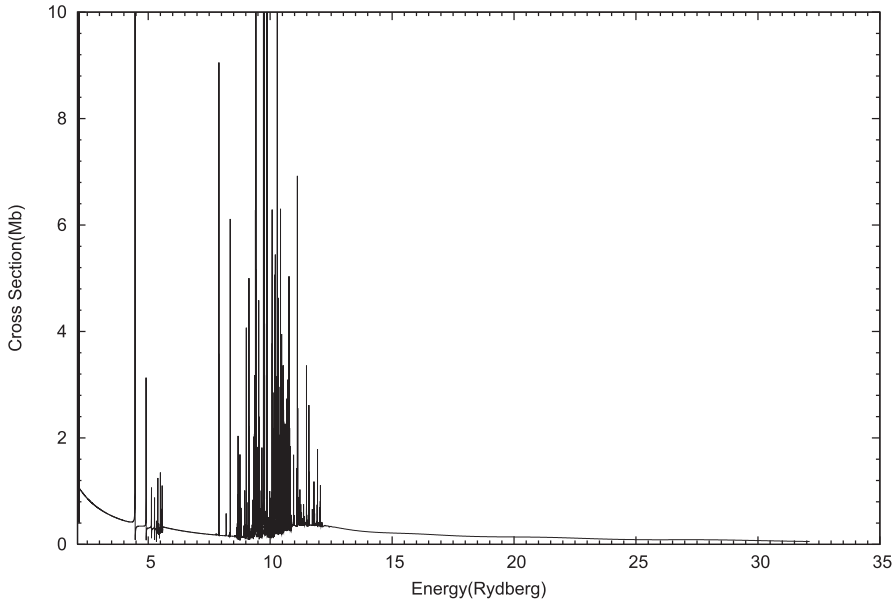

Fig. 5. Photoionization cross-section in Mb for the photoionization from $2s^2 2p^5(^2\mathrm{P}^\circ)3p\ ^1\mathrm{S}_0$ state of Al IV in Relativistic LSJ coupling as a function of photon energy in the full range upto 35 Rydberg.

significantly affect the photoionization cross-section. A three level calculation gives little indication of the complexity of the cross-section, particularly for the excited states, since it converges only $\Delta n = 0$ core excitation and coupling that are responsible for resonance [37]. The $\Delta n > 0$ couplings can be much stronger and give rise to more extensive resonances as shown in Figure 4 and as evident from target states given in Table 2.

Lastly, we have performed a relativistic R-matrix calculation to determine the cross-section for the photoionization of Al IV. Our new extensive calculations using the lowest 68 target levels of Al V are presented for the first time, to best of our knowledge, and should provide reasonably complete database for practical application for photoionization cross-section for Al IV. The averaging over resonances between the adjacent thresholds has not much advantage and so not considered in our calculations, as we have discussed different resonance series in detail. We expect our results to be quite reliable, as we have taken all the important physical effects like exchange, channel coupling and short-range correlation and relativistic effects [27] into account.

M.M. is thankful to DST (India) and UGC (India) for financial support. A.K.S.J. is thankful to DST for junior research fellow.

References

1. S.N. Nahar, Phys. Rev. A **69**, 042714 (2004); U. Feldman, G.A. Doschek, J.F. Seely, Mon. Not. R. Astron. Soc. **212**, 41 (1985); M.J. Seaton, J. Phys. B **20**, 6387 (1987); Y. Yan, M.J. Seaton, J. Phys. B **20**, 6409 (1987); G. Peach, H.E.

Saraph, M.J. Seaton, J. Phys. B **21**, 3669 (1988); D. Luo, A.K. Pradhan, J. Phys. B **22**, 3377 (1989)
2. K.A. Berrington, P.G. Burke, K. Butler, M.J. Seaton, P.J. Storey, K.T. Taylor, Yan Yu, J. Phys. B: At. Mol. Phys. **20**, 6379 (1987)
3. K.A. Berrington, P.G. Burke, M. Le Dourneuf, W.D. Robb, K.T. Taylor, Ky Vo Lan, Comput. Phys. Commun. **14**, 367 (1978)
4. K.A. Berrington, W.B. Eissner, P.H. Norrington, Comput. Phys. Commun. **92**, 290 (1995)
5. P.G. Burke, W.D. Robb, Adv. At. Mol. Phys. **11**, 143 (1975)
6. I.C. Lyon, B. Peart, K. Dolder, J.B. West, J. Phys. B: At. Mol. Phys. **20**, 1471 (1987)
7. I.C. Lyon, B. Peart, B.J. West, K. Dolder, J. Phys. B: At. Mol. Phys. **19**, 4137 (1986)
8. S.S. Tayal, P.G. Burke, J. Phys. B: At. Mol. Phys. **20**, 4715 (1987)
9. J.B. West, T. Andersen, R.L. Brooks, F. Folkmann, H. Kjeldsen, H. Knudsen, Phys. Rev. A **63**, 052719 (2001)
10. C.E. Hudson, J.B. West, K.L. Bell, A. Aguilar, R.A. Phaneuf, F. Folkmann, H. Kjeldsen, J. Bozek, A.S. Schlachter, C. Cisneros, J. Phys B: At. Mol. Opt. Phys. **38**, 2911 (2005)
11. H.S. Chakraborty, A. Gray, J.T. Costello, P.C. Deshmukh, G.N. Haque, E.T. Kennedy, S.T. Manson, J.P. Mosnier, Phys. Rev. Lett. **83**, 2151 (1999)
12. A.G. Kochur, D. Petrini, E.P. da Silva, A&A **393**, 1081 (2002)
13. V. Kaufman, M.C. Artu, W.L. Brillet, J. Opt. Soc. Am. **64**, 197 (1974)
14. M.C. Artru, V.J. Kaufman, Opt. Soc. Am. **65**, 594 (1975)
15. J. Soderqvist, Nova Acta Regiae, Soc. Sci. Ups., Ser. IV **9**, 1 (1934)
16. G. Jamelot, A. Sureau, P. Jaegle, Phys. Lett. A **41**, 153 (1972)
17. A. Carillon, G. Jamelot, A. Sureau, P. Jaegle, Phys. Lett. A **38**, 91 (1972)
18. S.O. Kastner, A.M. Crooker, W.E. Behring, L. Cohen, Phys. Rev. A **16**, 577 (1977)
19. V. Kaufman, M.C. Artru, W.U.L. Brillet, J. Opt. Soc. Am. **64**, 197 (1974); W.U.L. Brillet, Phys. Scripta **13**, 289 (1976); M. Eidelberg, M.C. Artru, Phys. Scripta **16**, 109 (1977); E.Ya. Kononov, A.E. Karmida, L.I. Podobedova, E.N. Ragozin, V.A. Chirkov, Phys. Scripta **28**, 496 (1983); C. Jupen, Nucl. Instrum. Meth. **202**, 25 (1982); M.C. Buchet-Poulizac, J.P. Buchet, Phys. Scripta **27**, 99 (1983)
20. B.C. Fawcett, Phys. Scripta **30**, 326 (1984)
21. J. Soderqvist, Nova Acta Regiae Soc. Sci. Ups., Ser. IV **9**, 1 (1934); E. Ferner, Ark. Mat. Astron. Fys. **36**, 1 (1948)
22. M.C. Artru, W.L. Brillet, J. Opt. Soc. Am. **64**, 1063 (1974)
23. W.L. Brillet, M.C. Artu, J. Opt. Soc. Am. **65**, 1399 (1975)
24. B. Rahmani, S.Y. Liu, K. Yasuoka, H.A. Belbachir, S. Ishii, Can. J. Phys. **77**, 994 (1999)
25. J. Nilsen, J. Quant. Spectrosc. Radiat. Transfer **47**, 171 (1992)
26. A. Hibbert, M.P. Scott, J. Phys. B **27**, 1315 (1994)
27. M. Mohan, K.L. Baluja, A. Hibbert, K.A. Berrington, Mon. Not. R. Astron. Soc. **225**, 337 (1989); M. Mohan, K.L. Baluja, A. Hibbert, Phys. Scripta **40**, 53 (1990); M. Mohan, M. Le Dourneuf, Astron. Astr. Phys. **227**, 285 (1990); M. Mohan, M. Le Dourneuf, Phys. Rev. A **41**, 2862 (1990); M. Mohan, M. Le Dourneuf, A. Hibbert, K.A. Berrington, Mon. Not. R. Astron. Soc. **243**, 372 (1990); M. Mohan, A. Hibbert, A.E. Kingston, Astrophys. J. **434**, 389 (1994)
28. M. Mohan, A. Hibbert, Phys. Scripta **44**, 158 (1991)
29. A. Hibbert, M. Mohan, M. Le Dourneuf, At. Nucl. Data Tables **53**, 23 (1993)
30. E. Clementi, C. Roetti, At. Data Nucl. Data Tables **14**, 177 (1974)
31. H.M.S. Blackford, A. Hibbert, At. Data Nucl. Data Tables **58**, 101 (1994)
32. NIST At. Spec. Database website `http://physics.nist.gov/cgi-bin/Atdata/level-form`
33. N. Verma, A.K.S. Jha, M. Mohan, J. Phys. B: At. Mol. Opt. Phys. **38**, 3185 (2005); N. Verma, A.K.S. Jha, M. Mohan, APJS **164**, 297 (2006); M. Mohan, A.K. Singh, A.K.S. Jha, P. Jha, At. Data Nucl. Data Table (in press); N. Singh, A.K.S. Jha, M. Mohan, Eur. Phys. J. D **38**, 285 (2006)
34. N.S. Scott, P.G. Burke, J. Phys. B **13**, 4299 (1980); P.G. Burke, K.T. Taylor, J. Phys. B **8**, 2620 (1975)
35. E.P. Winger, L. Eisenbud, Phys. Rev. **72**, 29 (1947)
36. M. Mohan, M. Le. Dourneuf, A. Hibbert, P.G. Burke, Phys. Rev. A **57**, 3489 (1998)
37. H.L. Zhang, S.N. Nahar, A.K. Pradhan, Phys. Rev. A **64**, 032719 (2001)